

# METHOD FOR PROBABILISTIC EVALUATION OF SEISMIC STRUCTURAL DAMAGE

By Ajay Singhal<sup>1</sup> and Anne S. Kiremidjian<sup>2</sup>

**ABSTRACT:** This paper presents a systematic approach for estimating fragility curves and damage probability matrices for different structural systems. Both fragility curves and damage probability matrices express the probabilities that a structure will sustain different degrees of damage at given ground motion levels. In contrast to previous approaches, this paper presents a method that is based on nonlinear dynamic analysis of the structure rather than on heuristics or on empirical data. The ground motion level for fragility curves is characterized by spectral acceleration. For damage probability matrices, modified Mercalli intensity is used as the ground motion parameter. The probabilities associated with the different damage states at a specified ground motion level are evaluated using the Monte Carlo-simulation technique. The nonstationary autoregressive moving average (ARMA) model is used for the generation of earthquake time histories. The approach presented in this paper is used to obtain fragility curves and damage probability matrices for reinforced concrete frames. Three different classes of reinforced concrete frames, based on the number of stories, are considered. Park and Ang's damage index is used to identify the different degrees of damage.

## INTRODUCTION

Information on structural damage is of critical importance for reliable economic loss evaluation for a structure or a region that has been or that might be affected by an earthquake. The extent of structural damage is also important in determining expected casualties from collapsed buildings or from falling debris. Relationships between earthquake ground motion severity and structural damage are most frequently used to characterize the damage distribution over a region. These motion-damage relationships are in the form of probability distributions of damage at specified ground motion intensities and are usually expressed by means of fragility curves or damage probability matrices (DPMs). Currently there are only two studies that provide damage probability matrices (ATC-13 1985), and fragility curves ("Development" 1995) for a wide variety of structural classes. The damage probability matrices in ATC-13 (1985) are based on expert opinion since actual damage data are very limited. The fragility curves in the standardized earthquake loss estimation methodology ("Development" 1995) are based on test data interpretation and judgment.

Fragility curves and damage probability matrices describe the conditional probabilities of sustaining different degrees of damage at given levels of ground motion. Thus, the development of fragility curves and damage probability matrices requires the characterization of the ground motion and the identification of the different degrees of structural damage. Earthquake ground motion amplitude, frequency content, and strong motion duration are some important characteristics that affect structural response and damage. Thus, they need to be taken into consideration in the development of fragility curves and DPMs.

This paper presents a systematic approach for developing damage-motion relationships that does not rely either on heuristics or on empirical data. Instead, the probability of damage is estimated by quantifying the response of a structure sub-

jected to a significant ensemble of ground motion with a wide range of parameter variations. For this purpose, a Monte Carlo-simulation approach is used to determine the probabilities of structural damage, and the ensemble of ground motions is generated using an autoregressive moving average (ARMA) model. The method is used to develop fragility curves and damage probability matrices for three categories of concrete frame structures. These include low-rise concrete frames that are one to three stories tall, mid-rise frames that are four to seven stories tall, and high-rise frames that are eight stories or taller. This classification is consistent with that defined in ATC-13 (1985) and is similar to that used in the standardized earthquake loss estimation methodology ("Development" 1995). The ground motion for these three classes of frames is characterized by spectral acceleration,  $S_a$ , over period bands corresponding to the three classes of frames. Similarly, damage probability matrices are developed for the same three classes of structures.

## METHODOLOGY

Ground-motion-versus-damage relationships characterize the level of damage to a particular class of structure as a function of a ground motion parameter. To represent the variability in earthquake ground motion and uncertainties in structural behavior, these relationships are most frequently described in the form of probabilities of damage conditional on the ground motion parameter. The two most widely used forms of motion-damage relationships are fragility curves and damage probability matrices.

A fragility curve describes the probability of reaching or exceeding a damage state at a specified ground motion level. Thus, a fragility curve for a particular damage state is obtained by computing the conditional probabilities of reaching or exceeding that damage state at various levels of ground motion. A plot of the computed conditional probabilities versus the ground motion parameter describes the fragility curve for that damage state. The conditional probabilities are defined as follows:

$$P_{ik} = P[D \geq d_i | Y = y_k] \quad (1)$$

where  $P_{ik}$  = probability of reaching or exceeding damage state  $d_i$  given that ground motion is  $y_k$ ;  $D$  = damage random variable defined on damage state vector  $\mathbf{D} = \{d_0, d_1, \dots, d_n\}$ ; and  $Y$  = ground motion random variable.

The damage states can be defined to characterize the physical state of the structure. A numerical damage scale in terms of the ratio of repair cost to replacement value of the structure

<sup>1</sup>Doctoral Candidate, The John A. Blume Earthquake Engrg. Ctr., Dept. of Civ. Engrg., Stanford Univ., Stanford, CA 94305-4020.

<sup>2</sup>Prof. and Dir., The John A. Blume Earthquake Engrg. Ctr., Dept. of Civ. Engrg., Stanford Univ., Stanford, CA.

Note. Associate Editor: Bilal M. Ayyub. Discussion open until May 1, 1997. To extend the closing date one month, a written request must be filed with the ASCE Manager of Journals. The manuscript for this paper was submitted for review and possible publication on December 9, 1994. This paper is part of the *Journal of Structural Engineering*, Vol. 122, No. 12, December, 1996. ©ASCE, ISSN 0733-9445/96/0012-1459-1467/\$4.00 + \$.50 per page. Paper No. 9754.

can also be specified. The different damage measures and their segregation into damage states are discussed later in the paper. Several different parameters have been used to describe the ground motion. In this study, the average spectral acceleration,  $S_a$ , over a specified structural period range will be used. However, the methodology can be used with many different earthquake ground motion parameters, such as root-mean-square (RMS) acceleration.

Another commonly used representation of structural damage as a function of the earthquake ground motion is the damage probability matrix. A damage probability matrix specifies the discrete probabilities of reaching a damage state at different ground motion levels. These probabilities are defined as follows:

$$p_{ik} = P[D = d_i | Y = y_k] \quad (2)$$

where  $p_{ik}$  = probability of reaching damage state  $d_i$  given that ground motion is  $y_k$ .

In this paper, modified Mercalli intensity (MMI) is used as the ground motion parameter for the damage probability matrices. For that purpose, relationships between MMI and spectral acceleration are developed in the relevant period band. The formulation for obtaining the damage probability matrices is shown as follows:

$$P_{D|MMI}[d|MMI] = \int_{S_a} P_{D|MMI,S_a}[d|MMI, S_a] f_{S_a|MMI}[S_a|MMI] dS_a \quad (3)$$

where  $P_{D|MMI}[d|MMI]$  = probability of reaching or exceeding given damage state at specified MMI;  $P_{D|MMI,S_a}[d|MMI, S_a]$  = probability of reaching or exceeding given damage state at specified MMI and spectral acceleration; and  $f_{S_a|MMI}[S_a|MMI]$  = conditional probability density function of spectral acceleration at specified MMI, obtained by assuming this distribution to be lognormal with parameters determined later in paper. The previous formulation can be simplified by assuming that the probability of reaching or exceeding a given damage state at specified MMI and spectral acceleration is the same as the probability of reaching or exceeding a given damage state at specified spectral acceleration. It should be recognized that both spectral acceleration and MMI are used as ground motion parameters. Thus, representing the probability of damage as a function only of spectral acceleration should not have a significant effect on the results. This assumption can be verified as additional data become available. Eq. (3) can then be simplified as follows:

$$P_{D|MMI}[d|MMI] = \int_{S_a} P_{D|S_a}[d|S_a] f_{S_a|MMI}[S_a|MMI] dS_a \quad (4)$$

Kiremidjian (1985) presented a method for developing motion-damage relationships by using consensus probability distributions of damage obtained from subjective probability densities provided by individual experts. Fragility formulations have been developed and used extensively for components and mechanical assemblies in nuclear power plant safety analyses (Kennedy et al. 1980; Kennedy and Ravindra 1984). For building systems, fragility formulations have been presented by Hwang and Jaw (1990) and Hwang and Huo (1994), the ground motion being characterized by peak ground acceleration. It has been shown by many researchers that peak ground acceleration is a very poor indicator of damage. Furthermore, the simulated time histories that Hwang and Jaw (1990) and Hwang and Huo (1994) used for developing the fragility curves for buildings are stationary in their frequency content. Yeh and Wen (1990) showed that the nonstationarity in frequency content has a significant effect on the response of non-

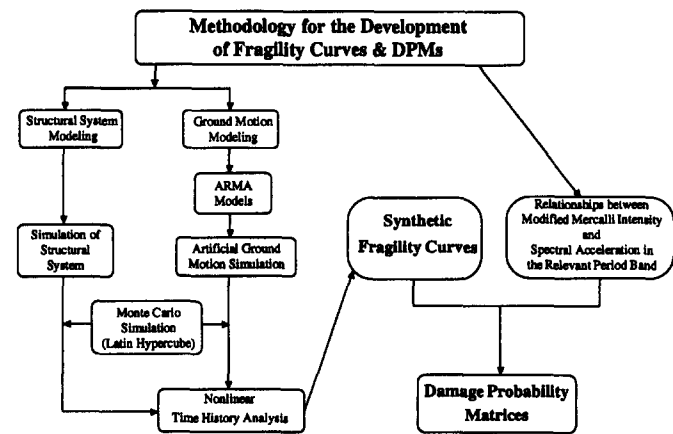


FIG. 1. Steps in Development of Fragility Curves and Damage Probability Matrices

linear systems. The present study incorporates nonstationarity in both the amplitudes and the frequency content of the ground motion. Also, this study adopts spectral acceleration to characterize ground motion.

The major components of the methodology presented in this paper consist of (1) characterization of the structure when subjected to extreme dynamic loads; (2) characterization of the potential ground motions; and (3) quantification of the structural response that includes the variability in the ground motion and the uncertainty in the structural parameters. It is difficult to develop analytical closed-form solutions for motion-damage relationships because neither the ground motion nor the nonlinear behavior of the structure can be described in an analytical form. Thus, a Monte Carlo simulation approach is used to estimate the probabilities of damage conditional on different ground motion levels. The general framework of this methodology is described in Fig. 1.

Damage to structures subjected to severe earthquake ground shaking depends on their dynamic characteristics and their nonlinear behavior. This evaluation of damage requires that nonlinear dynamic analyses be performed for a wide range of earthquake ground motion time histories. For the nonlinear dynamic analysis, it is necessary that the hysteretic behavior of structural components be specified. When fragility curves are needed for many different classes of structures, the structural properties need to be representative of a wide range of structures that can fall within that specified structural category. For this purpose, it is proposed that a generic structure be designed for a specified structural system reflecting a particular design code specification. The behavior of individual structures is likely to differ from the behavior of the generic structure used in the development of the fragility curves. However, the damage estimated from the generic structure is expected, on the average, to be representative over the range of different structures within this structural class.

### Characterization of Ground Motion

To characterize earthquake ground motion for the purposes of evaluating structural performance, it is necessary to describe the amplitude, frequency content, and duration of ground motion. The input energy of earthquake ground motion can be represented as the sum of the kinetic energy, the damping energy, the irrecoverable hysteretic energy, and the recoverable elastic strain energy of a structure. The spectral velocity values at different periods provide an estimate of the maximum kinetic energy imparted by the earthquake to an elastic single-degree-of-freedom (SDOF) system at those periods. For an undamped, elastic SDOF system, the maximum kinetic energy is equal to the input energy of the earthquake ground motion.

The pseudo-spectral velocity can easily be related to the pseudo-spectral acceleration by the period of the SDOF system at which these two quantities are computed. The spectral acceleration values are used in this paper to specify different levels of ground motion when developing motion-damage relationships in the form of fragility curves. For the damage probability matrices, MMI is used to identify the different levels of ground motion, as has traditionally been done. The relationship between these parameters needs to be investigated. This relationship will be investigated in the application of the method to concrete frame structures.

The spectral values at different periods are frequently represented by means of dynamic amplification factors. The dynamic amplification factors represent the normalized spectral values at specified damping, obtained as a ratio of the spectral acceleration to the peak ground acceleration. Fig. 2 shows the dynamic amplification factors obtained at a damping ratio of 5% of the critical damping from 68 firm sites of the Loma Prieta, Whittier Narrows, and Morgan Hill earthquakes. Kirimidjian and Shah (1980) demonstrated the applicability of the lognormal distribution to dynamic amplification factors. We verified the lognormal distribution by applying the Kolmogorov-Smirnov analysis to the dynamic amplification factors shown in Fig. 2 at periods of 0.5, 1.0, 1.5, and 2.0 s. Although the average spectral shapes shown in Fig. 2 appear to be smooth in each period band, the individual time histories may have sharp peaks in their spectra. Our interest, however, is in the average response of the structures over all of the time histories. Since a structure is likely to be subjected to many different ground motions during its service life, it is important to consider an ensemble of ground motions that have a wide range of characteristics.

The strong motion duration is another ground motion characteristic that influences damage. Jeong and Iwan (1988) show that duration can have a strong influence on the expected damage of a structure. Several measures of strong motion duration have been discussed in the literature [e.g., Bolt (1973); Trifunac and Brady (1975); Vanmarcke and Lai (1980); McCann and Shah (1979)]. Trifunac and Brady's (1975) definition of strong motion duration is used in this paper because of its computational simplicity. The start and end of the Trifunac and Brady strong motion are the times to accumulate 5% and 95% of the total energy, respectively.

Furthermore, earthquake ground motion time histories are needed for the analysis. If a large sample of earthquake ground motion time histories that cover all the different parameter ranges is available, then these time histories can be discriminated according to distance to the fault, local soil parameters, and spectral characteristics, and then can be used for the dynamic analysis of the structure and the evaluation of the fragility curves. Such a consistent ensemble of time histories is

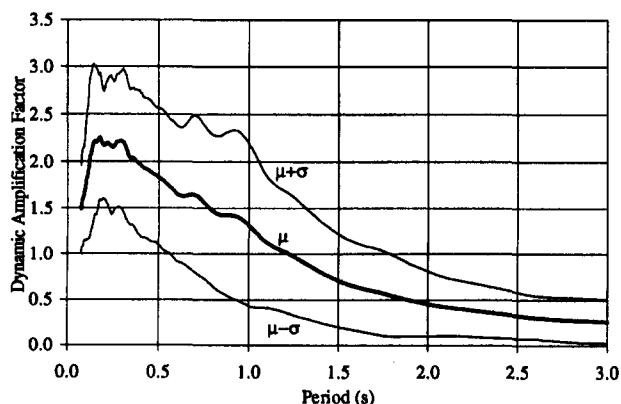


FIG. 2. Dynamic Amplification Factors at 5% of Critical Damping for Ground Motions Recorded on Firm Sites

not currently available, even though there are a large number of recordings obtained from recent earthquakes. Thus, it is proposed that ensembles of time histories be simulated at each specified ground motion parameter level.

Several procedures are available for the generation of artificial time histories. These include stationary Gaussian models with modulating functions and ARMA models. Liu and Jhaveri (1969) and Vanmarcke (1976) proposed Gaussian models with modulating functions, among many others. Deodatis and Shinozuka (1989) developed a stochastic wave model with evolutionary power to simulate ground motion. This model is useful for simulating ground motions for large scale structures where spatial variation of ground motion is important. ARMA models have been used for the generation of artificial ground motion time histories by many researchers including Polhemus and Cakmak (1981) and Conte et al. (1992). To capture the nonstationarity in the frequency content of the ground motion, nonstationary ARMA models are used to simulate time histories in the present study.

The stationary ARMA model of order  $(p, q)$  is represented by the following equation:

$$a_k - \phi_1 a_{k-1} - \dots - \phi_p a_{k-p} = e_k - \theta_1 e_{k-1} - \dots - \theta_q e_{k-q} \quad (5)$$

where  $a_k = a(k\Delta t)$ ,  $k = 0, 1, 2, \dots$  = discrete stationary correlated process;  $e_k = e(k\Delta t)$  = zero-mean Gaussian white-noise process with variance  $\sigma_e^2$ ;  $\Delta t$  = sampling time interval;  $\phi_i$ ,  $i = 1, \dots, p$  = autoregressive parameters; and  $\theta_i$ ,  $i = 1, \dots, q$  = moving average parameters. A special case of the ARMA( $p, q$ ) model is the ARMA(2, 1) model. This model is completely defined by the two autoregressive parameters, the moving average parameter, and the variance of the white noise process. Conte et al. (1992) show that the ARMA(2, 1) processes can be interpreted as the response processes of linear, viscously damped SDOF systems.

Recorded earthquake time histories exhibit nonstationarities in amplitude and frequency content. To incorporate these two nonstationarities, a dynamic version of the ARMA model is used. This model is represented by the following equation:

$$a_k - \phi_{1,k} a_{k-1} - \dots - \phi_{p,k} a_{k-p} = e_k - \theta_{1,k} e_{k-1} - \dots - \theta_{q,k} e_{k-q} \quad (6)$$

The nonstationarity in amplitude is represented by the variance envelope of the underlying white-noise process,  $\sigma_{e,k}^2$ , and the nonstationarity in frequency content is modeled by the time varying ARMA parameters,  $\phi_{i,k}$  and  $\theta_{i,k}$ . The uncoupling of these two nonstationarities is possible if the standard deviation envelope,  $\sigma_{e,k}$ , is slowly varying in time compared to the periods of the earthquake motion.

In this study, the moving time-window technique is used to estimate the ARMA parameters of recorded ground motions from the Loma Prieta, Whittier Narrows, and Morgan Hill earthquakes. The moving window assumes that the time history is stationary within a time window. The program MATLAB (MATLAB 1994) is used to estimate the ARMA parameters within each window. The ARMA parameters estimated for each window are assumed to be representative of the center point of the window. The parameter estimation is repeated for successive equidistant window positions. Based on a parametric study conducted to estimate the size of the ARMA model and the window size, it was found that the ARMA(2, 1) model with a window size of 3 s gives reasonable results in terms of the spectral acceleration of the simulated time histories. The window is moved by 0.2 s between successive window positions. When generating time histories for a particular level of spectral acceleration, each simulated time history is scaled to match the desired spectral acceleration.

RMS acceleration is used to normalize the spectral shapes.

RMS acceleration is insensitive to isolated peaks in the ground motion and is an average statistic for the entire time history. RMS acceleration is defined as

$$\sigma_0 = \left[ \frac{1}{T_s} \int_{T_s} a^2(t) dt \right]^{1/2} \quad (7)$$

where  $\sigma_0$  = RMS of strong-motion acceleration;  $T_s$  = strong-motion duration; and  $a(t)$  = ground motion acceleration at time  $t$ . Fig. 3 presents a comparison of the mean normalized spectral shapes computed from recorded time histories, obtained from the Loma Prieta, Whittier Narrows, and Morgan Hill earthquakes and an ensemble of simulated time histories.

As strong motion duration is an important ground motion characteristic that affects damage to structures, it is worthwhile to examine the distribution of strong motion duration for the recorded ground motion from which the ARMA parameters are estimated. A lognormal probability distribution function with median = 11.22 s and  $\sigma_{\ln(T_s)} = 0.310$  s is found to fit the observed distribution, as shown in Fig. 4.

### Characterization of Damage

There are several quantitative damage measures that characterize the state of structures after earthquakes. Most of the definitions consider damage to individual elements and are based on ductility ratio or dissipated energy (Banan et al. 1981). Examples of damage indices for reinforced concrete structures include those by Park et al. (1984), Chung et al. (1989), and DiPasquale and Cakmak (1990). The Krawinkler index (Krawinkler 1987) is a measure frequently used to quantify damage in steel components.

For reinforced concrete structures, the Park and Ang (1985a,b) model has been widely used in recent years because

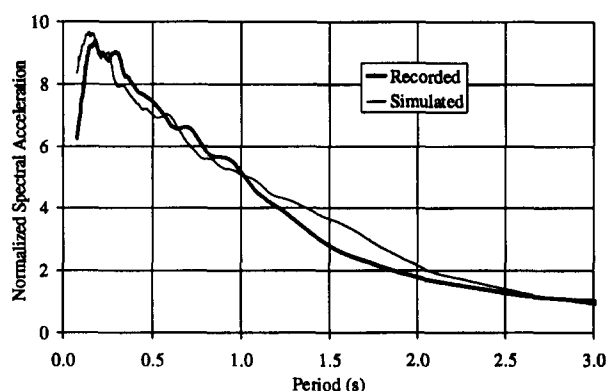


FIG. 3. Comparison of Ensemble Means from Recorded and Simulated Time Histories

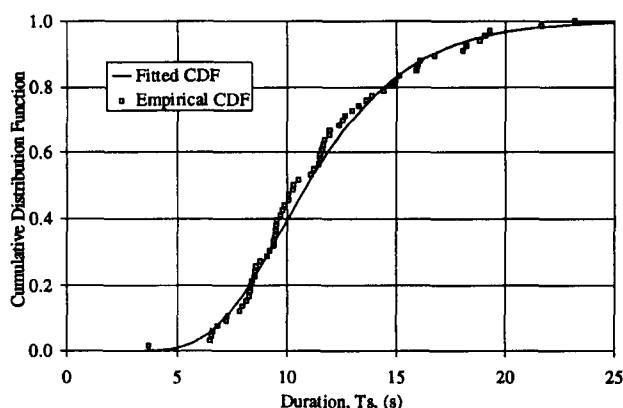


FIG. 4. Lognormal Cumulative Distribution Function of Strong Motion Duration

it is simple and because it has been calibrated using data from various structures damaged during past earthquakes. An equivalent form of the Park and Ang index is used in this paper. For a structural component, the index is defined as follows:

$$D = \frac{\theta_m}{\theta_u} + \frac{\beta}{M_y \theta_u} \int dE \quad (8)$$

where  $\theta_m$  = maximum positive or negative plastic hinge rotation;  $\theta_u$  = plastic hinge rotation capacity under monotonic loading;  $\beta$  = model parameter (0.15 in this paper);  $M_y$  = calculated yield strength; and  $dE$  = incremental dissipated hysteretic energy.

The first term in (8) represents the damage due to maximum deformation experienced during cyclic loading. The second term represents the damage due to cumulative hysteretic energy dissipation. The damage index,  $D$ , is 0 when there is no damage and is 1.0 for collapse. Cosenza et al. (1990) found that the value of  $\beta = 0.15$  correlates closely with results based on other damage models. Thus, this value of  $\beta$  is used in the present study.

Park and Ang's (1985b) global damage index is used to represent the performance of structural systems. It is defined as a weighted average of the local damage indices of each element. The weighting function for each element is proportional to the energy dissipated in the element. The global damage index is given by the following equation:

$$D_T = \sum \lambda_i D_i \quad (9a)$$

where

$$\lambda_i = \frac{E_i}{\sum E_i}; E_i = \text{energy dissipated at location } i \quad (9b)$$

In addition to the overall damage index, story-level damage indices can also be obtained. The overall structure damage indices are used in this paper for the identification of the different damage states of concrete structural frames. For other structures, appropriate quantitative damage measures need to be defined.

To estimate economic loss or casualties as a result of structural damage, the structural damage must be expressed in terms of discrete damage states. Discrete damage states allow the damage sustained by a structure to be expressed in terms of the nature and extent of the damage suffered by its components. Thus, structural damage, which is a continuous function of building response, is quantified by discrete damage states. The five discrete damage states used in this paper are none, minor, moderate, severe, and collapse. To obtain these discrete damage states, ranges for the damage measures mentioned earlier need to be specified.

In the present study, the different damage states of a concrete building are identified based on the Park-Ang global damage indices of the overall structure. Park et al. (1984) calibrated the damage index with the observed damage to nine reinforced concrete buildings caused by different earthquakes. The report by Park et al. (1987) gives the semantic definitions for the ranges of damage corresponding to different values of the Park and Ang damage index. Gunturi (1992) further investigated these damage states and simplified them according to his findings. Further calibration of the Park-Ang damage index was performed by De Leon and Ang (1994) using data from eight reinforced concrete buildings that sustained different levels of damage during the 1985 Mexico City earthquake. Stone and Taylor (1994) also calibrated the Park-Ang damage index based on an extensive study of reinforced concrete columns. The ranges of the Park and Ang index for different damage states have been established to reflect damage to concrete frames more realistically and are presented in Table 1.

**TABLE 1. Ranges of Park and Ang's Damage Index for Different Damage States**

Damage state (1)	Range of the Park and Ang index (2)
Minor	0.1–0.2
Moderate	0.2–0.5
Severe	0.5–1.0
Collapse	>1.0

### Fragility and DPM Simulation

To estimate the damage to structures, it is necessary to model the uncertainties associated with structural capacities and demands. Structural capacities and demands can be characterized by a number of parameters that have an important effect on the response statistics and overall reliability of the system. Structural capacities are defined in terms of the capacities of members as part of the structure. Much greater uncertainty is associated with seismic demands than with other demands on the structure. Artificial ground motion simulation is carried out to incorporate the uncertainty in seismic demands. The ARMA(2, 1) model described earlier in this paper is used for the simulation of ground motion time histories. In this paper, the variabilities associated with structural capacities and demands are treated independently.

The fragility formulation defined in (1) is determined by the Monte Carlo-simulation method. The Monte Carlo-simulation technique involves the selection of values of the input random variables required for nonlinear dynamic analyses. Examples of input random variables to model capacities for reinforced concrete structures include the strengths of steel and concrete. Latin hypercube sampling provides a good method for selecting the values of the input random variables. In this paper, 100 Latin hypercube samples are used for the nonlinear dynamic analysis at each ground motion level. From the simulations, the means, variances, and distribution functions of the output random variable, the quantitative measure of damage in our case, are estimated for an ensemble of time histories corresponding to a given level of ground motion. The probabilities of different damage states are evaluated from the probability distributions of the damage measure. The damage probability matrices are evaluated from the fragility curves by using (4).

### APPLICATION OF METHOD TO REINFORCED CONCRETE FRAMES

To illustrate the method for fragility and DPM development, sample buildings in the three classes of reinforced concrete frames are considered. The evaluation of the damage probability matrices from the fragility curves is based on the relationship between the MMI and the spectral acceleration developed and presented in this paper.

The average spectral acceleration ordinate in the period range corresponding to the three classes of reinforced concrete frames is used to characterize the ground motion for fragility curves. The three period bands used in this paper are 0.1–0.5 s, 0.5–0.9 s, and 0.9–2.5 s. These period bands are based on the study reported in "NEHRP" (1992) and are estimated to reflect the natural periods of buildings belonging to the three classes of reinforced concrete frames. Artificial time histories are simulated corresponding to a specified value of average spectral acceleration.

### Modeling of Uncertainties in Structural Capacities and Demands

The structural capacities and demands need to be specified stochastically before the Monte Carlo simulation can be per-

formed. The following two sections discuss the uncertainties associated with the capacity and demand parameters for reinforced concrete frames.

### Capacity Parameters

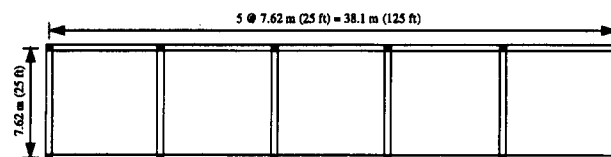
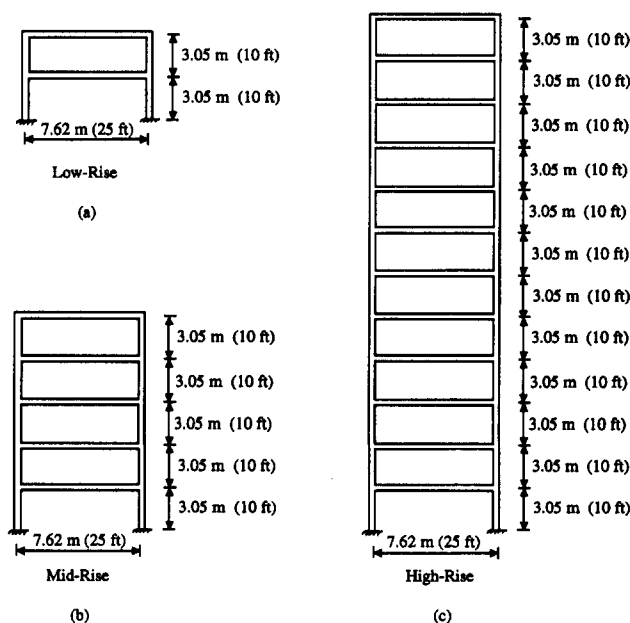
The parameters that affect the resistance of the structure include the compressive strength of concrete, the yield strength of reinforcing steel, hysteretic behavior, damping ratio, physical dimensions of the different components, and the amount of reinforcing steel. The compressive strength of concrete and the yield strength of steel are the only parameters treated as the strength random variables in this paper. Following Galambos et al. (1982), the writers use a normal probability distribution for concrete strength and a lognormal probability distribution for steel strength. Concrete strength has a mean of 1.14 times the nominal concrete strength and a coefficient of variation of 0.14. Steel strength has a mean of 1.05 times the nominal strength and a coefficient of variation of 0.11.

### Demand Parameters

In this paper, only the earthquake load is modeled as a nonstationary stochastic process. The nonstationary ARMA(2, 1) model is used for simulating 100 artificial time histories. Each generated time history is scaled to match the average spectral acceleration over the period band corresponding to a particular class of reinforced concrete frames.

### Description of Sample Structures

The example structures are considered to have five bays in the longitudinal direction and one bay in the transverse direction. The sample building for each class of concrete frames is designed according to the 1990 SEAOC Recommendations (Recommended 1990) for special moment resisting frames.

**FIG. 5. Plan View of Sample Structures****FIG. 6. Elevations of Sample Frames for Three Classes: (a) Low-Rise Frame; (b) Mid-Rise Frame; (c) High-Rise Frame**

The thickness of the floor slab in these buildings is assumed to be 17.78 cm (7 in.). A uniformly distributed dead load of 1.44 kPa (30 psf) is superimposed on the self weight of the structure and is used in the design of the members. In addition, reduced live loads for member design were represented by a uniformly distributed load of 1.44 kPa (30 psf). The plans of the three structures are the same and the plan of a typical structure is shown in Fig. 5. A typical interior frame for each of the three structures was used in the nonlinear time history analysis to estimate damage at different levels of ground shaking. Based on FEMA 223 ("NEHRP" 1992), a story height of 304.8 cm (10 ft) is used for these buildings. Fig. 6 shows the elevations for the three frames used in the analysis.

### Sample Fragility Curves

The computer programs IDARC2D (Kunnath and Reinhorn 1994) and DRAIN-2DX (Prakash and Powell 1992) are used for damage analysis. The member properties in terms of moment-rotation relationships are evaluated in IDARC2D. These properties are then used for the nonlinear dynamic analyses performed in DRAIN-2DX. The spread of plasticity along the length of each member is captured by a discretization of the member into smaller elements. Based on a parametric study, one small element of length equal to 15% of the member length at each end along with a larger middle element are able to incorporate the spread of plasticity along the member length satisfactorily. The details of this parametric study will be published in a subsequent paper.

Different elements of a structure are expected to behave nonlinearly when subjected to severe ground motion. A hysteretic relationship is used to describe the nonlinear behavior in terms of the restoring force and the member deformation. The program DRAIN-2DX used for the nonlinear analysis in this study has a bilinear hysteretic model with no degradation in strength or stiffness. Nonlinear dynamic analyses are performed for 100 artificial ground motions generated at each value of spectral acceleration. An integration time step of 0.002 s is used in the analyses. The damping matrix was obtained as a linear combination of the mass and stiffness matrices. The coefficients for the mass and stiffness matrices were selected to give 5% of critical damping in the first two vibrational modes. The Park-Ang damage index given by (8) and (9) is computed from the results of the time history analysis performed in DRAIN-2DX.

The statistics of the Park and Ang damage index, obtained at each spectral acceleration value, are used to obtain the parameters of a lognormal probability distribution function at that ground motion level. Figs. 7–9 show the comparison between the empirical probability distributions obtained from simulation results and the fitted lognormal distributions at

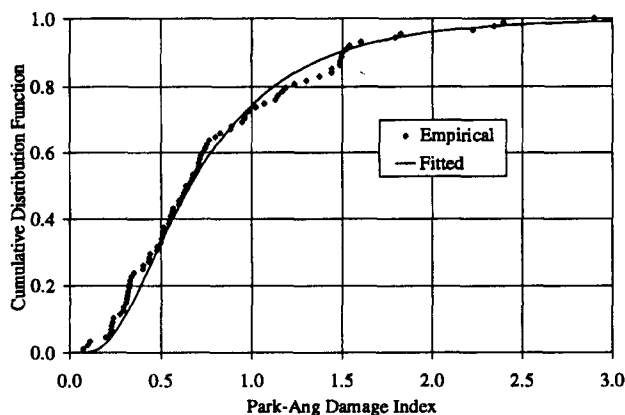


FIG. 7. Comparison of Probability Distributions for Low-Rise Frame at  $S_a = 4g$

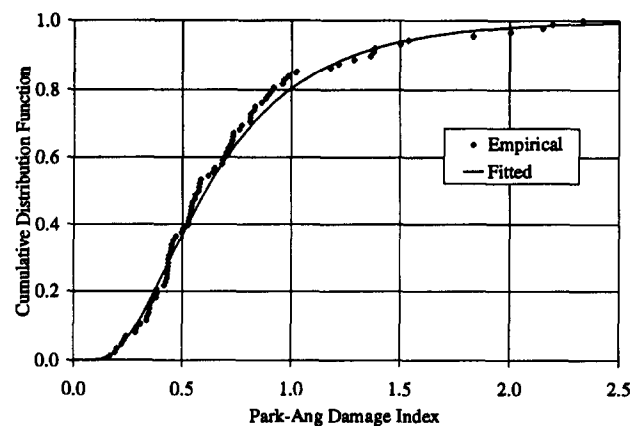


FIG. 8. Comparison of Probability Distributions for Mid-Rise Frame at  $S_a = 3g$

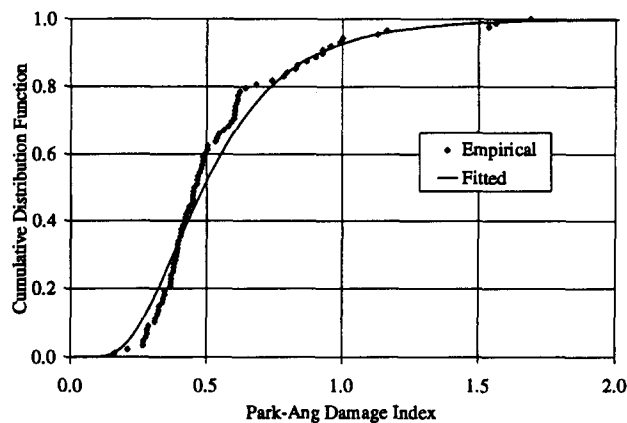


FIG. 9. Comparison of Probability Distributions for High-Rise Frame at  $S_a = 1.5g$

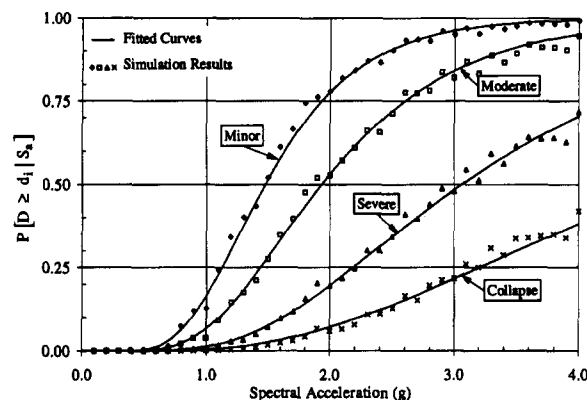


FIG. 10. Fragility Curves for Sample Low-Rise Building

spectral acceleration values of 4g, 3g, and 1.5g, respectively. The Kolmogorov-Smirnov test is used, and these lognormal distributions are verified at a 5% significance level.

The lognormal probability functions at each level of ground motion are then used to obtain the probabilities of reaching or exceeding a damage state. The threshold values for the different damage states are given in Table 1. Smooth fragility curves are obtained by arbitrarily fitting lognormal distribution functions to the simulation results. The simulation results and the fitted curves are shown as discrete points and smooth curves, respectively, in Figs. 10–12.

### Sample Damage Probability Matrices

The relationship between the MMI and the average spectral acceleration in each period band is investigated in order to

obtain the damage probability matrices from the fragility curves using the formulation of (4). The average spectral acceleration values of the ground motions recorded on firm sites and the MMI values from these earthquakes at the respective recording stations are used to develop these relationships. The firm site records of the Loma Prieta, Whittier Narrows, and Morgan Hill earthquakes are used for estimating the relationship between the average spectral acceleration and MMI. The larger of the two horizontal components of ground motion at a site is used in evaluating this relationship.

The average spectral acceleration in each period range is assumed to have a conditional lognormal probability density function at given values of MMI. Regression analysis is performed between the natural logarithm of the mean of the average spectral acceleration and MMI. Similar regression analysis is performed between the standard deviation of the average spectral acceleration and MMI. The resulting regression curves are used to estimate the means and standard de-

viations of the average spectral acceleration at higher MMI values for which observed data are not available. The regression equations for the mean and standard deviation of the average spectral acceleration, expressed in  $\text{cm/s}^2$  in each period band, are shown as follows:

$$\mu_{S_a|MMI} = 7.49e^{0.59MMI} \quad \text{for } 0.1 \leq T \leq 0.5 \quad (10)$$

$$\sigma_{S_a|MMI} = 16.35e^{0.41MMI} \quad \text{for } 0.1 \leq T \leq 0.5 \quad (11)$$

$$\mu_{S_a|MMI} = 2.78e^{0.68MMI} \quad \text{for } 0.5 \leq T \leq 0.9 \quad (12)$$

$$\sigma_{S_a|MMI} = 5.95e^{0.52MMI} \quad \text{for } 0.5 \leq T \leq 0.9 \quad (13)$$

$$\mu_{S_a|MMI} = 0.31e^{0.85MMI} \quad \text{for } 0.9 \leq T \leq 2.5 \quad (14)$$

$$\sigma_{S_a|MMI} = 1.54e^{0.55MMI} \quad \text{for } 0.9 \leq T \leq 2.5 \quad (15)$$

The curves representing the mean values, mean plus and minus one standard deviation values, and the median values of the average spectral acceleration are shown in Figs. 13–15. These figures also show the conditional distributions for the average spectral acceleration, with MMI in the 5–8 range.

The integral in (4) is evaluated numerically by using the subroutine QDAGI in *IMSL* (1991). This subroutine uses a 21-point Gauss-Kronrod rule to estimate the integral. The probability of the structure being in a particular damage state, at a specified MMI, is estimated by taking the difference in probabilities of two adjacent damage states evaluated by means of (4). For example, the probability of the structure being in moderate damage state is given by the probability of the structure reaching or exceeding the severe damage state minus the probability of the structure reaching or exceeding the moderate damage state. These probabilities are computed at the ground motion level of interest.

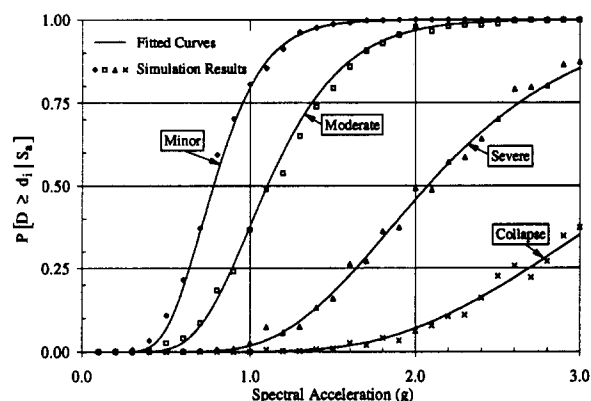


FIG. 11. Fragility Curves for Sample Mid-Rise Building

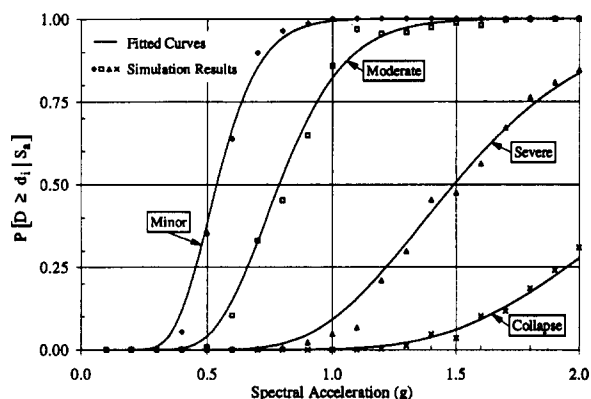


FIG. 12. Fragility Curves for Sample High-Rise Building

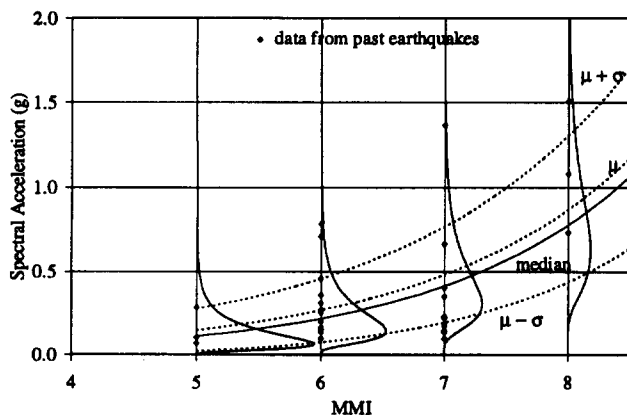


FIG. 13.  $S_a$ -MMI Correlation and Probability Distributions for Spectral Acceleration Averaged over Period Range 0.1–0.5 s

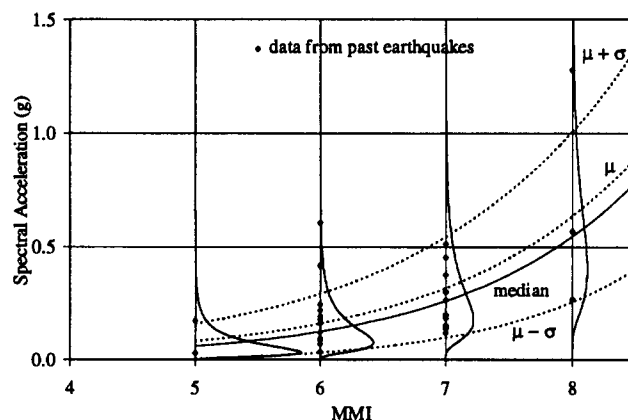


FIG. 14.  $S_a$ -MMI Correlation and Probability Distributions for Spectral Acceleration Averaged over Period Range 0.5–0.9 s

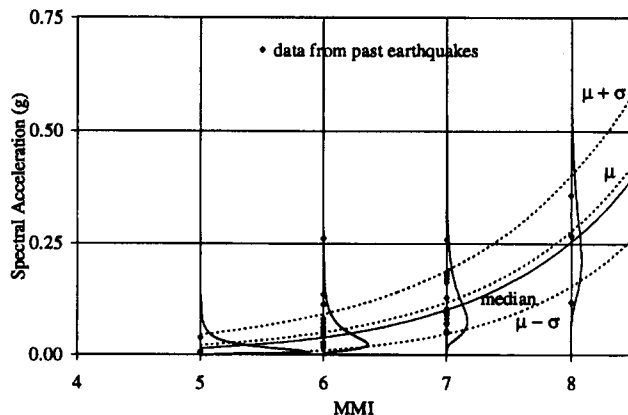


FIG. 15.  $S_a$ -MMI Correlation and Probability Distributions for Spectral Acceleration Averaged over Period Range 0.9–2.5 s



Tables 2–4 show the damage probability matrices evaluated for the representative buildings. These matrices show an increase in the probability of the collapse damage state at higher MMI values as the building height is increased. The collapse damage state as defined by Park et al. (1987) includes total or partial collapse of the building. Thus, as the building height is increased, it is reasonable to expect the probability of partial collapse anywhere in the building to increase.

The damage probability matrices of *ATC-13* (1985) were transformed to correspond to the damage states used in this paper. Tables 5–7 present the transformed damage probability matrices for ductile reinforced concrete frames. It is observed that the damage probability matrices of *ATC-13* are confined to a narrow band, whereas the damage probability matrix from this study has a larger bandwidth. Moreover, the damage probability matrices of *ATC-13* show much less damage at higher levels of MMI. This may be due to some differences in the definitions of damage states used in *ATC-13* and in the current study. The negligible probability of collapse of the frames at MMI values of 11 and 12 given in *ATC-13* appear rather unrealistic, particularly in view of the performance of concrete

**TABLE 2. Damage Probability Matrix for Sample Low-Rise Building**

Damage state (1)	Modified Mercalli Intensity						
	VI (2)	VII (3)	VIII (4)	IX (5)	X (6)	XI (7)	XII (8)
None	99.5	97.0	85.4	52.9	14.1	0.9	—
Minor	0.3	1.6	6.9	16.9	15.5	3.4	0.1
Moderate	0.2	1.1	5.4	18.5	30.5	17.6	2.8
Severe	—	0.2	1.4	7.0	20.7	28.0	14.6
Collapse	—	0.1	0.9	4.7	19.2	50.1	82.5

**TABLE 3. Damage Probability Matrix for Sample Mid-Rise Building**

Damage state (1)	Modified Mercalli Intensity						
	VI (2)	VII (3)	VIII (4)	IX (5)	X (6)	XI (7)	XII (8)
None	99.0	93.5	70.0	24.5	1.6	—	—
Minor	0.7	4.2	15.8	23.0	6.1	0.1	—
Moderate	0.3	2.1	12.0	36.6	33.7	4.9	0.2
Severe	—	0.2	1.9	12.5	34.6	22.3	1.8
Collapse	—	—	0.3	3.4	24.0	72.7	98.0

**TABLE 4. Damage Probability Matrix for Sample High-Rise Building**

Damage state (1)	Modified Mercalli Intensity						
	VI (2)	VII (3)	VIII (4)	IX (5)	X (6)	XI (7)	XII (8)
None	100.0	99.7	93.0	35.3	0.2	—	—
Minor	—	0.3	5.7	35.3	3.3	—	—
Moderate	—	—	1.3	26.9	45.9	0.7	—
Severe	—	—	—	2.4	38.9	11.8	—
Collapse	—	—	—	0.1	11.7	87.5	100.0

**TABLE 5. *ATC-13* (1985) Damage Probability Matrix for Low-Rise, Ductile Moment Resisting Frames**

Damage state (1)	Modified Mercalli Intensity						
	VI (2)	VII (3)	VIII (4)	IX (5)	X (6)	XI (7)	XII (8)
None	2.5	—	—	—	—	—	—
Minor	97.5	100.0	99.6	63.2	7.3	0.1	—
Moderate	—	—	0.4	36.8	92.7	99.9	99.5
Severe	—	—	—	—	—	—	0.5
Collapse	—	—	—	—	—	—	—

**TABLE 6. *ATC-13* (1985) Damage Probability Matrix for Mid-Rise, Ductile Moment Resisting Frames**

Damage state (1)	Modified Mercalli Intensity						
	VI (2)	VII (3)	VIII (4)	IX (5)	X (6)	XI (7)	XII (8)
None	0.3	—	—	—	—	—	—
Minor	99.7	99.8	91.8	46.7	9.0	—	—
Moderate	—	0.2	8.2	53.3	91.0	100.0	99.6
Severe	—	—	—	—	—	—	0.4
Collapse	—	—	—	—	—	—	—

**TABLE 7. *ATC-13* (1985) Damage Probability Matrix for High-Rise, Ductile Moment Resisting Frames**

Damage state (1)	Modified Mercalli Intensity						
	VI (2)	VII (3)	VIII (4)	IX (5)	X (6)	XI (7)	XII (8)
None	—	—	—	—	—	—	—
Minor	100.0	100.0	83.6	27.6	3.1	0.4	0.1
Moderate	—	—	16.4	72.4	96.9	99.2	96.4
Severe	—	—	—	—	—	0.4	3.5
Collapse	—	—	—	—	—	—	—

frame structures in recent large earthquakes. It is also possible that the spectral accelerations predicted at higher MMI using the MMI-spectral acceleration relationships developed earlier may be exaggerated due to the fact that the relationships are derived using observations at lower MMI values. Ground motion recordings at larger MMI values are needed in order to accurately predict the spectral acceleration values at higher MMI levels.

## SUMMARY AND CONCLUSIONS

This paper presents a systematic approach for developing damage-motion relationships that does not rely either on heuristics nor on empirical data. Instead, the probability of damage to a structure is estimated by a Monte Carlo-simulation approach. Ideally, such curves should be verified with observed damage data. However, such data are very limited and are usually not in the proper format to allow either the generation or the verification of fragility curves for all structural classes and all ground motion levels. As more data are collected in a systematic manner, such verification and empirical analysis will become possible.

The uncertainties in the ground motion were modeled by generating artificial time histories using the nonstationary ARMA model. The parameters of the ARMA model were estimated from the firm site records of the Loma Prieta, Whittier Narrows, and Morgan Hill earthquakes. This paper also develops a formulation for estimating the damage probability matrices from the fragility curves. The relationship between MMI and the average spectral acceleration was investigated in order to obtain the damage probability matrices from the fragility curves.

The method developed in this paper is used to obtain fragility curves and damage probability matrices for reinforced concrete frames. These fragility curves and damage probability matrices consider the nonlinear properties of the structure and the nonstationary characteristics of the ground motions. Thus, they represent the most consistent set of fragility curves and DPMs currently available and can be used for estimating damage states for a wide range of reinforced concrete frames. Furthermore, the damage estimates can be used for cost-benefit analysis purposes in retrofit decisions and in the evaluation of potential losses to concrete frames over a region.

In general, it is desirable to obtain fragility curves for all structural classes. Furthermore, the effect of structural char-



acteristics not included in this study also need to be investigated. For example, three-dimensional, nonlinear dynamic analyses need to be performed in order to study the effect of plan irregularity on the damage to the structure. The effect of elevation irregularities should also be investigated. A considerable amount of computational effort is required to perform nonlinear dynamic analyses for estimating damage. Thus, procedures for obtaining the fragility curves with reduced computational effort need to be investigated.

## ACKNOWLEDGMENTS

This research is currently supported by NCEER contract 92-4101. Their continued funding is appreciated. The writers express their gratitude to Dr. Andrei Reinhorn for providing the program IDARC2D, and to Dr. S. K. Kunnath for responding to various queries on IDARC2D. The writers also express their thanks to Dr. J. P. Conte for providing input on ARMA modeling of ground motions.

## APPENDIX. REFERENCES

- ATC-13: *earthquake damage evaluation data for California*. (1985). Applied Technology Council, Redwood City, Calif.
- Banon, H., Biggs, J. M., and Irvine, H. M. (1981). "Seismic damage in reinforced concrete frames." *J. Struct. Engrg.*, ASCE, 107(9), 1713–1729.
- Bolt, B. A. (1973). "Duration of strong ground motions." *Proc., 5th World Conf. on Earthquake Engrg.*, 1, 1304–1313.
- Chung, Y. S., Meyer, C., and Shinozuka, M. (1989). "Modeling of concrete damage." *ACI Struct. J.*, 86(3), 259–271.
- Conte, J. P., Pister, K. S., and Mahin, S. A. (1992). "Nonstationary ARMA modeling of seismic motions." *Soil Dyn. and Earthquake Engrg.*, 11, 411–426.
- Cosenza, E., Manfredi, G., and Ramasco, K. (1990). "An evaluation of the use of damage functionals in earthquake-resistant design." *Proc., 9th Eur. Conf. on Earthquake Engrg.*, The Kucherenko Tsniisk of the USSR, Gosstroy, Moscow, 9, 303–312.
- De Leon, D., and Ang, A. H-S. (1994). "A damage model for reinforced concrete buildings: further study with the 1985 Mexico City earthquake." *Proc., 6th Int. Conf. on Struct. Safety and Reliability*, A. A. Balkema, Rotterdam, The Netherlands, 3, 2081–2087.
- Deodatis, G., and Shinozuka, M. (1989). "Simulation of seismic ground motion using stochastic waves." *J. Engrg. Mech.*, ASCE, 115(12), 2723–2737.
- "Development of a standardized earthquake loss-estimation methodology." (1995). Draft Tech. Manual 100% Submittal, Prepared for Nat. Inst. of Build. Sci., Risk Management Solutions, Inc., Menlo Park, Calif.
- DiPasquale, E., and Cakmak, A. S. (1990). "Seismic damage assessment using linear models." *Soil Dyn. and Earthquake Engrg.*, 9(4), 194–215.
- Galambos, T. V., Ellingwood, B., MacGregor, J. G., and Cornell, C. A. (1982). "Probability based load criteria: assessment of current design practice." *J. Struct. Div.*, ASCE, 108(5), 959–977.
- Gunturi, S. K. (1992). "Building specific earthquake damage estimation," PhD thesis, Stanford Univ., Stanford, Calif.
- Hwang, H. H. M., and Huo, J-R. (1994). "Generation of hazard consistent fragility curves." *Soil Dyn. and Earthquake Engrg.*, 13, 345–354.
- Hwang, H. H. M., and Jaw, J-W. (1990). "Probabilistic damage analysis of structures." *J. Struct. Engrg.*, ASCE, 116(7), 1992–2007.
- IMSL *User's Manual*. (1991). The International Mathematical and Statistical Library, IMSL, Inc., Houston, Tex.
- Jeong, G. D., and Iwan, W. D. (1988). "The effect of earthquake duration on the damage of structures." *Earthquake Engrg. and Struct. Dyn.*, 16, 1201–1211.
- Kennedy, R. P., Cornell, C. A., Campbell, R. D., Kaplan, S., and Perla, H. F. (1980). "Probabilistic seismic safety study of an existing nuclear power plant." *Nuclear Engineering and Design*, North-Holland Publishing Co., Amsterdam, Holland, 315–338.
- Kennedy, R. P., and Ravindra, M. K. (1984). "Seismic fragilities for nuclear power plant risk studies." *Nuclear Engineering and Design*, North-Holland Publishing Co., Amsterdam, Holland, 47–68.
- Kiremidjian, A. S. (1985). "Subjective probabilities for earthquake damage and loss." *Struct. Safety*, 2, 309–317.
- Kiremidjian, A. S., and Shah, H. C. (1980). "Probabilistic site-dependent response spectra." *J. Struct. Engrg.*, ASCE, 106(1), 69–86.
- Krawinkler, H. (1987). "Performance assessment of steel components." *Earthquake Spectra*, 3(1), 27–41.
- Kunnath, S. K., and Reinhorn, A. M. (1994). "IDARC2D version 3.1: inelastic damage analysis of RC buildings." Dept. of Civ. Engrg., State Univ. of New York at Buffalo.
- Liu, S. C., and Jhaveri, D. P. (1969). "Spectral simulation and earthquake site properties." *J. Engrg. Mech. Div.*, ASCE, 95(5), 1145–1168.
- MATLAB—*system identification toolbox user's guide*. (1994). The Mathworks, Inc., Natick, Mass.
- McCann, M. W., and Shah, H. C. (1979). "Determining strong-motion duration of earthquakes." *Bull. Seismological Soc. of Am.*, 69(4), 1253–1265.
- "NEHRP recommended provisions for the development of seismic regulations for new buildings: part 2—commentary." (1992). FEMA 223. *Earthquake Hazards Reduction Series 65*, Fed. Emergency Mgmt. Agency, Washington, D.C.
- Park, Y-J., Ang, A. H-S., and Wen, Y. K. (1984). "Seismic damage analysis and damage-limiting design of R.C. buildings." *Struct. Res. Ser. Rep. No. UILU-ENG-84-2007*, Univ. of Illinois at Urbana-Champaign, Urbana, Ill.
- Park, Y-J., and Ang, A. H-S. (1985a). "Mechanistic seismic damage model for reinforced concrete." *J. Struct. Engrg.*, ASCE, 111(4), 722–739.
- Park, Y-J., and Ang, A. H-S. (1985b). "Seismic damage analysis of reinforced concrete buildings." *J. Struct. Engrg.*, ASCE, 111(4), 740–757.
- Park, Y-J., Reinhorn, A. M., and Kunnath, S. K. (1987). "IDARC: inelastic dynamic analysis of reinforced concrete frame-shear-wall structures." *Tech. Rep. NCEER-87-0008*, Nat. Ctr. for Earthquake Engrg. Res., State Univ. of New York, Buffalo, N.Y.
- Polhemus, N. W., and Cakmak, A. S. (1981). "Simulation of earthquake ground motions using autoregressive moving average (ARMA) models." *Earthquake Engrg. and Struct. Dyn.*, 9, 343–354.
- Prakash, V., and Powell, G. H. (1992). *DRAIN-2DX: user's guide*. Dept. of Civ. Engrg., Univ. of California at Berkeley.
- Recommended lateral force requirements and commentary*. (1990). Struct. Engrs. Assn. of California.
- Rubinstein, R. Y. (1981). *Simulation and the Monte Carlo method*. John Wiley & Sons, Inc., New York, N.Y.
- Stone, W. C., and Taylor, A. W. (1994). "ISDP: integrated approach to seismic design of reinforced concrete structures." *J. Struct. Engrg.*, ASCE, 120(12), 3548–3566.
- Trifunac, M. D., and Brady, A. G. (1975). "A study on the duration of strong earthquake ground motion." *Bull. Seismological Soc. of Am.*, 65(3), 581–626.
- Vanmarcke, E. H. (1976). "Structural response to earthquakes." *Seismic risk and engineering decisions*, C. Lomnitz and E. Rosenblueth, eds., Elsevier Publishing Company Inc., New York, N.Y., 287–337.
- Vanmarcke, E. H., and Lai, S-S. P. (1980). "Strong-motion duration and RMS amplitude of earthquake records." *Bull. Seismological Soc. of Am.*, 70(4), 1293–1307.
- Yeh, C. H., and Wen, Y. K. (1990). "Modeling of nonstationary ground motion and analysis of inelastic structural response." *Struct. Safety*, 8, 281–298.